Journal of The Electrochemical Society, **160** (10) A1629-A1637 (2013)
0013-4651/2013/160(10)/A1629/9/$31.00 © The Electrochemical Society

Fast Charge/Discharge of Li Metal Batteries Using an Ionic Liquid Electrolyte

H. Yoon,[a,b] P. C. Howlett,[c] A. S. Best,[b,z] M. Forsyth,[c,*] and D. R. MacFarlane[a]

[a]*School of Chemistry, Monash University, Victoria 3800, Australia*
[b]*Commonwealth Scientific and Industrial Research Organisation (CSIRO), Division of Energy Technology, Clayton, Victoria 3169, Australia*
[c]*ARC Centre of Excellence for Electromaterials Science (ACES), Institute for Frontier Materials (IFM), Deakin University, Burwood, Victoria 3125, Australia*

Because of their potentially superior safety characteristics, room temperature ionic liquids (RTILs or ILs) have been vigorously researched as a potential replacement for current commercial lithium battery electrolytes, which are based on volatile and flammable organic carbonates. However, relatively poor battery performance, which is a consequence of the higher viscosity and lower conductivity of these materials, has prevented them becoming mainstream electrolytes for commercial lithium batteries. Amongst various RTILs, those containing the bis(fluorosulfonyl)imide (FSI) anion exhibit high conductivities and diffusivities, making them interesting potential electrolytes for lithium metal batteries. Here, we evaluate the electrochemical stability, lithium electrochemistry, and Li^+ transference numbers of FSI-based ionic liquid electrolytes intended for use in rechargeable Li metal batteries. We show that ILs containing high concentrations of lithium, up to 3.2 mol.kg^{-1} in C_3mpyr FSI, have excellent rate capability (higher than that of standard battery electrolytes) with both the lithium metal electrode and $LiCoO_2$ cathode, in spite of their significantly higher viscosities and lower conductivities. This unusual behavior is ascribed to the concomitant increase in transference number with increasing Li-salt concentration.
 [DOI: 10.1149/2.022310jes]

Manuscript submitted April 1, 2013; revised manuscript received July 17, 2013. Published July 26, 2013.

The challenge to develop suitable electrolytes having wide electrochemical windows and high Li^+ transference number for lithium-ion batteries has become increasingly important as applications require increases in capacity, charging rate and safety.[1] Room Temperature Ionic Liquids (RTILs or ILs) are potential candidates as electrolytes. These materials came to prominence in the late 1990's as solvents suitable for electrochemical reactions and over the last 15 years, there have been many studies on ILs for battery applications, as evidenced by significant numbers of patents and publications.[2,3] These materials have numerous features that should lend themselves for use in high energy lithium batteries: negligible volatility, relatively high decomposition temperatures when compared to traditional lithium battery electrolytes, high ionic conductivity and wide electrochemical windows.[4–6]

Of all anions to date, the sulfonylimide family are the most studied, and show, in general, the best electrochemical performance. ILs containing the bis(fluorosulfonyl)imide (FSI) anion exhibit higher conductivities and diffusivities than the corresponding bis(trifluoromethanesulfonyl)imide (TFSI or NTf_2) compounds, thereby generating interest as potential electrolytes for lithium metal batteries.[7–16] However, there are several aspects of concern, including high temperature stability and corrosion.[17–19]

The Li salt concentration in an IL is important for charging and discharging of Li batteries, because in general, while increasing the Li salt concentration increases the viscosity and decreases the conductivity, it also increases the amount of lithium ions available in the IL.[20] Seki et al. studied the effect of LiTFSI salt concentrations (from 0 to 0.8 mol.kg^{-1}) on the performance of 1,2-dimethyl-3-propylimidazolium bis(trifluoromethylsulfonyl)imide (DMPImTFSI). They measured conductivity, viscosity, electrochemical impedance spectra (EIS) and the rate capability of a $LiCoO_2$ cathode based cell, and found that the optimum salt concentration was 0.4 mol.kg^{-1}.[20]

In most commercial lithium-ion batteries, a concentration of 0.8 to 1.2 M Li salt in organic liquid electrolyte is used to maximize cell performance by achieving a balance between conductivity and viscosity. Nyman et al. confirmed this optimum concentration effect in an organic liquid electrolyte by measuring both conductivities and transference numbers.[21]

Following Zhou et al.'s electrochemical and physicochemical studies on *N*-propyl-*N*-methylpyrrolidinium bis(fluorosulfonyl)-imide (C_3mpyr FSI) and *N*-butyl-*N*-methylpyrrolidinium bis(fluorosulfonyl)-imide (C_4mpyr FSI),[13] Paillard et al. added different amounts of LiFSI salts (mole ratios from 0 to 0.6, where a mole ratio of 0.6 LiFSI : 0.4 C_4mpyr is equivalent to an LiFSI concentration of 4.9 mol.kg^{-1}) to C_4mpyr FSI and performed physical and electrochemical studies.[14] Unlike previous reports showing that additional lithium salts increased the cathodic electrochemical stability in imidazolium-based TFSI ILs,[22,23] increasing the amount of LiFSI salts in C_4mpyr FSI decreased the cathodic stability in their study; this was attributed to the high level of impurities in the commercial grade LiFSI salt used.[14] They also demonstrated that the FSI anion (in contrast to the TFSI anion) could establish a solid electrolyte interphase (SEI) on graphite anodes without the need for additives. FSI may also allow the exploitation of the high voltage plateaus of materials such as $LiNi_{0.5}Mn_{1.5}O_2$ and $LiNi_{0.33}Mn_{0.33}Co_{0.33}O_2$, leading to higher energy lithium-ion batteries.[24–26] However, they did not explain the effect of lithium concentration on electrochemical and battery properties (other than the increased electrochemical window). Best and Bhatt studied various lithium salts in C_3mpyrFSI at concentrations ranging from 0.2 to 1 mol.kg^{-1}, and found that 0.5 mol.kg^{-1} $LiBF_4$ showed the widest electrochemical windows and Li symmetric cell stability.[15,27] They also studied the lithium electrochemistry of the FSI anion using cyclic voltammetry (CV) and EIS, and showed that these electrolytes can be used to cycle a Li metal anode.[15,27]

In this work, we examine the effects of salt concentration on various electrochemical properties of C_3mpyrFSI. In cycling lithium-metal symmetric cells as a function of lithium salt concentration, we show remarkably low cycling over-potentials at various current densities. We demonstrate that because of the C_3mpyr FSI IL's stability against lithium metal, the Bruce and Vincent method for measuring transference numbers can be effectively used to determine $t_{Li}{}^+$ without complications from the SEI layer. Finally, we show that ionic liquids based on C_3mpyr FSI with especially high concentrations of LiFSI are able to effectively cycle batteries consisting of lithium anodes and $LiCoO_2$ cathodes at high charge-discharge rates.

Experimental

Materials.— *N*-propyl-*N*-methylpyrrolidinium bis(fluorosulfonyl)imide (C_3mpyrFSI, purity > 99.9%) and lithium

*Electrochemical Society Active Member.
zE-mail: Adam.Best@csiro.au

Table I. Salt concentrations in each electrolyte.

LiFSI conc. in IL	Molar ratio of each ions		
(mol.kg^{-1})	Li^+	C_3mpyr^+	FSI^-
0 (neat IL)	0	0.50	0.50
0.8	0.10	0.40	0.50
1.6	0.17	0.33	0.50
2.4	0.21	0.29	0.50
3.2	0.25	0.25	0.50

bis(fluorosulfonyl)imide (LiFSI, purity > 99.5%) were both sourced from Suzhou Fluolyte Co., Ltd., China. The moisture content of all the electrolytes studied here were < 20 ppm, as determined via Karl Fisher titration (Metrohm). Lithium metal was sourced from China Energy Lithium Co., Ltd. (purity > 99.9%).

Electrolytes for these experiments were prepared by adding LiFSI to C_3mpyrFSI IL and stirring for 24 hours at room temperature in an Ar- filled glove box (< 5 ppm O_2 and H_2O). Table I shows the concentration of each electrolyte and molar ratio of each ion in solution. The highest Li salt concentration used in these experiments was 3.2 mol.kg^{-1}, which has an ion ratio of 1 Li^+: 1 C_3mpyr^+: 2 FSI^-.

Cyclic Voltammetry.— A 1 mm diameter Pt working electrode and a Pt wire counter electrode were employed for cyclic voltammetry and a 3 mm diameter Ni working electrode was also employed for comparison. The surface area (0.009 cm^{-2}) of the Pt electrode was obtained by measuring a bis(cyclopentadienyl)iron(II) (ferrocene, or Fc) Fc | Fc^+ redox peak currents determined using 5 mM Fc at scanning rates of 20, 50, 100 and 200 mV.sec^{-1}, and then applying the Randles-Sevcik equation.[28] The surface area of Ni working electrode was not measured but just calculated from the apparent diameter. The reference electrode consisted of a silver wire immersed in a solution of 10 mM silver triflate (AgTf, 99.95 + % purity, Aldrich) in *N*-butyl-*N*-methylpyrrolidinium bis(trifluoromethanesulfonyl)imide (C_4mpyr TFSI, Merck high purity specification, <100 ppm water, <100 ppm chloride) and separated from the main solution by a glass frit, as reported by Snook et al.[29] Therefore, the CV measurements were performed against Ag | Ag^+ reference potential and converted into Li | Li^+ redox potential. The potential was checked with a Fc | Fc^+ internal reference. The scan rate was 20 mV.s^{-1}. Measurements were obtained at 23 ± 3°C. Potentiostatic control was provided by an Autolab Pgstat302 (Eco Chimie, Netherlands) controlled with GPES (Version 4.9.005) software.

Coin cell preparation.— CR2032 size lithium symmetric cells were prepared with 2 10 mm^2 diameter lithium disks and a Solupor 7P03A separator (Lydall, Inc., UK) in an Ar-filled glove box. Cells were then stored for 24 hours at 50°C.

$LiCoO_2$ electrodes consisted of 90 wt% $LiCoO_2$ (Nippon Chemical Industrial, Japan), 5 wt% carbon black (Shawinigan) and 5 wt% PVdF binder. Dry ingredients were ball milled together for 72 h, prior to the addition of the binder (dissolved in *N*-methylpyrrolidone) to form a slurry. The slurry was ball milled for a further 72 h prior to being spread onto aluminum foil using a 60 μm graded roller. Coated foils were allowed to dry overnight in a fume hood and then dried further in a vacuum oven at 100°C for 72 h. The final $LiCoO_2$ loading was approximately 4.5 mg.cm^{-2}. $LiCoO_2$ cells were prepared with the electrodes, Li disks, and Solupor 7P03A separators (50 μm thick, micro-porous polyethylene). All cells were then stored for 24 hours at 50°C before cycling to allow for wetting. The specific capacities of the prepared electrodes were checked by making cells with a standard battery electrolyte (1M $LiPF_6$, EC:DMC = 50:50 vol.%, Mitsubishi Chemical Co.).

Transference number.— Lithium symmetrical cells were used to determine the Li^+ transference number with the method described by Evans, Bruce, and Vincent.[30,31]

Cells were polarized at 25°C with a constant voltage of 1.0 mV for 5 min. 10 min. 20 min. or 2 hours and the currents during the polarization were measured. The EIS spectra were measured before and after the polarization using a 1 mV perturbation. 24 hours recovery was allowed between each experiment. All experiments were conducted using a Solartron 1470 Battery test unit connected to a 1255B Frequency response analyser with Corrwave ver. 3.1c and Z-plot ver. 3.1c.

Coin cell cycling.— Li | $LiCoO_2$ cells were charged to 4.2 V and discharged to 2.75 V at 0.1 C, 0.5 C, 1.0 C, 1.5 C, 2.0 C, 3.0 C, 4.0 C or 5.0 C constant currents to measure charge and discharge rate capability, and then cycled at 0.1 C at 25°C on a Maccor Series 4000 instrument.

Results and Discussion

Cyclic Voltammetry.— Cyclic voltammograms (20 mV.sec^{-1} scan rate) are presented for LiFSI dissolved in C_3mpyrFSI at room temperature using mainly a Pt working electrode in Figure 1. It is known that a Pt working electrode forms an alloy with lithium during the reduction of lithium[32] while there is no alloy formation when using a Ni working electrode. For comparison purposes, we have embedded the Ni working electrode CVs in Figure 1a and 1d. In Figure 1a, the Li^+ reduction peak for 0.8 mol.kg^{-1} solution was observed at −3.77 V vs. Ag | Ag^+, and two distinct oxidation peaks were observed at −3.08 V and −2.08 V with the main Li stripping occurring at −3.08 V and successive Li under-potential deposition stripping and residual H_2O oxidation at higher potentials.[33]

When the salt concentration is increased to 1.6 mol.kg^{-1} (Figure 1b) the Li^+ deposition peak moves to a more negative potential, −3.87 V, while the corresponding Li stripping peak moves to a more positive potential, −2.91 V, because of the decreasing ionic conductivity and increasing viscosity of the electrolyte. This trend persists at even higher solution concentrations, as shown in Figure 1c and 1d. Unlike Paillard et al., we do not observe a large parasitic current prior to Li plating (which had been ascribed to the purity of the LiFSI salt).[14] Figure 1d and 1e show the electrochemistry at the highest salt concentration, 3.2 mol.kg^{-1}; in both cases, we do not observe a well-defined lithium deposition peak. We have first cycled the electrolyte to −5 V (Figure 1d) then to −6.5 V (Figure 1e) to find the lithium deposition peak. After scanning reductively to −6.5 V vs. Ag | Ag^+ (Figure 1e) a stripping peak is observed on the first cycle, however, because of coincident electrolyte decomposition and lithium deposition, the stripping peak current decreases rapidly, and the peak is no longer observable after 5 cycles. Whilst we do not observe a lithium deposition peak in Figure 1d, the cycling efficiency is significantly higher when cycled in this narrower electrochemical window. These two experiments allow us to determine that the bulk IL reduction process occurs between −5 and −6.5 V in the 3.2 mol.kg^{-1} electrolyte. Figure 1f shows that in all the solutions prepared here, the cathodic stability is unchanged by the presence of various concentrations of lithium salt. Finally, we note that the shift in the peak positions of the lithium deposition and stripping are also influenced by the speciation of Li in solution, as evidenced by the changing NMR ^{7}Li chemical shift. This effect will be described in more detail in a forthcoming paper.

Bhatt et al. reported that a salt concentration of 0.45 mol.kg^{-1} shows better cycling stability than 0.2 mol.kg^{-1}.[27] However, in this study, the lowest Li concentration in the IL is 0.8 mol.kg^{-1} and all electrolytes in Figures 1c to 1f show essentially stable lithium deposition and stripping for 5 cycles. Moreover, and very significantly, the lithium deposition current densities for the highest salt concentrations start at −30 mA.cm^{-2} (Figure 1d) and increases in magnitude to −80 mA.cm^{-2} (Figure 1e), equivalent to a 27A charge rate (or 7.5C rate) in a 18650 cell having 3.6 Ah capacity with 4 mAh.cm^{-2} loading on both sides of the Al current collector.[34] This shows the potential use of these electrolytes for fast charging lithium batteries. In addition, this trend also remains when using Ni working electrode. Figure 2

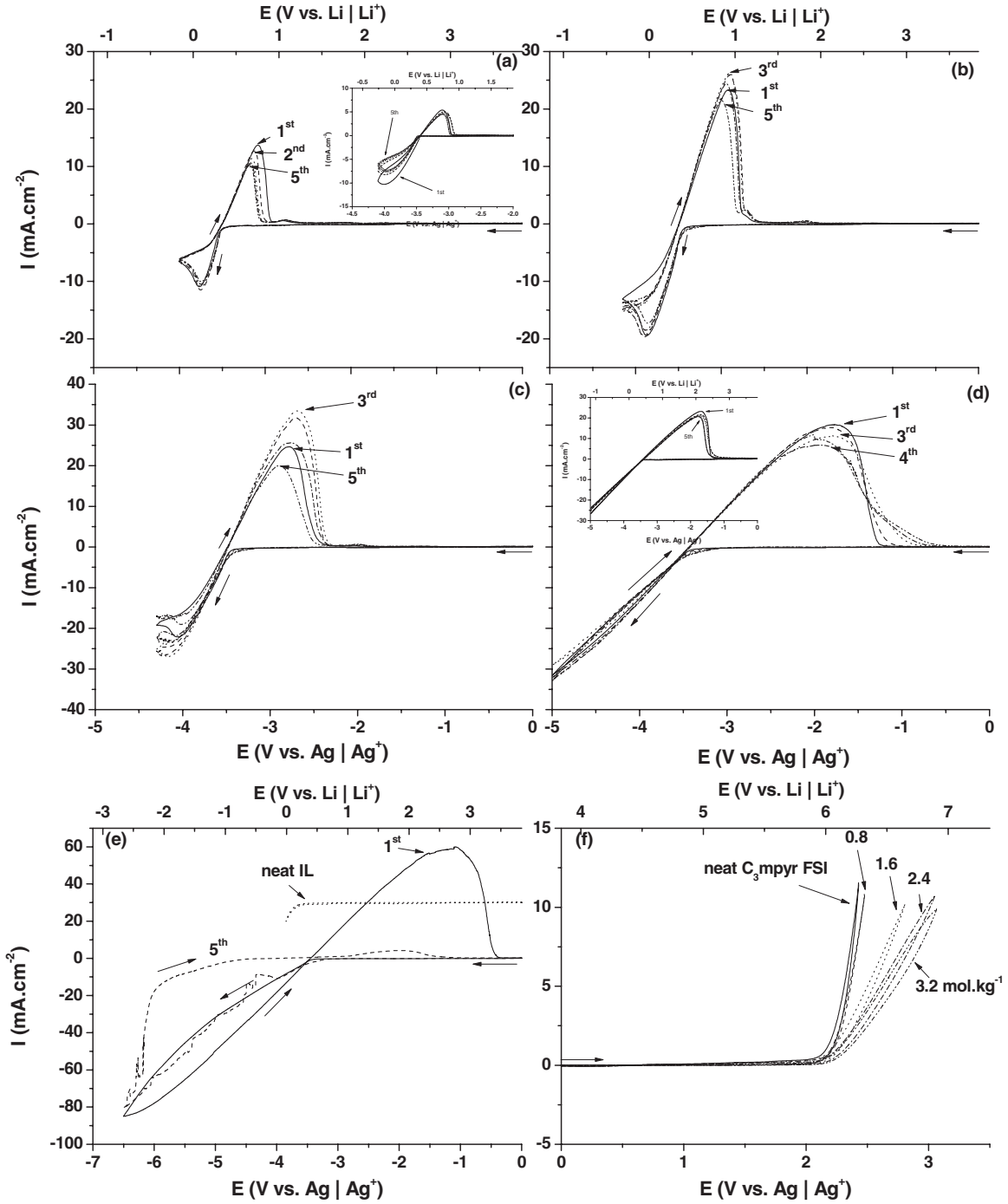

Figure 1. Cyclic voltammograms (Pt working electrode, 20 mV.sec^{-1}, room temperature) for concentrated LiFSI in C_3mpyrFSI ILs: a) 0.8 mol.kg^{-1}, b) 1.6 mol.kg^{-1}, c) 2.4 mol.kg^{-1},(d) 3.2 mol.kg^{-1} –5 V cutoff, (e) 3.2 mol.kg^{-1}, −6.5 V cutoff 1st cycle (solid line) and 5th cycle (dashed line) compared with the neat IL (dotted line, arbitrary current range), (f) Anodic electrochemical limits. The embedded boxes in the figure (a) and (d) are the CV with Ni working electrode. Note: Top axis is converted to the Li | Li$^+$ redox potential from Ag | Ag$^+$ potential (bottom).

shows the Li deposition and stripping efficiencies for the different salt concentrations studied in this work. The Coulombic efficiency is higher at concentrations such as 2.4 mol.kg^{-1} or 3.2 mol.kg^{-1}, which can be attributed to the high number of charge carriers in solution.

Cycling performance of C_3mpyrFSI lithium symmetrical coin cells.— We have constructed Li symmetrical cells to determine if the stability of Li cycling depends on the lithium salt concentration. These cells have been cycled at different current densities from 0.01 mA.cm^{-2} to 1 mA.cm^{-2}, at room temperature. The voltage-time responses for the different salt concentrations are shown in Figure 3. Each cell shows that, for any given applied current density, the overpotential remains relatively stable; the most significant changes occur with changes in salt concentration. The cell resistance increases with increasing molar concentrations of Li salt up to 2.4 mol.kg^{-1}, and then decreases when the salt concentration reaches 3.2 mol.kg^{-1}. The internal resistance values calculated from the DC polarizations are several hundred Ω.cm^{-2}, as expected from the resistivities of the electrolytes obtained from EIS measurements. When the polarization current density was increased to 0.1 mA.cm^{-2}, (Figure 3b) the same trend

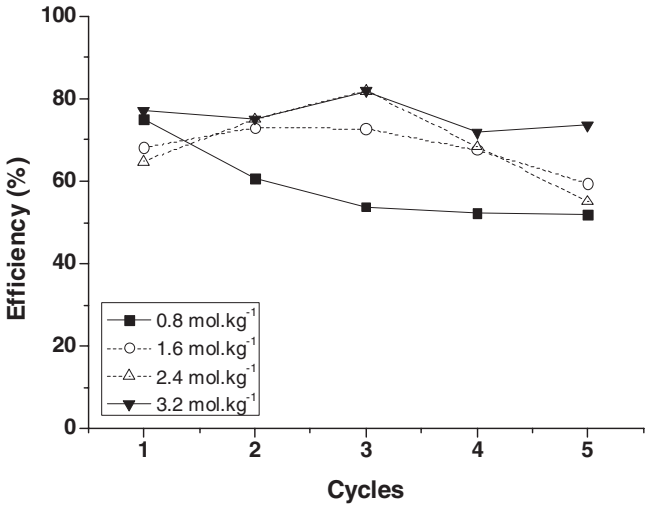

Figure 2. Li stripping/deposition columbic efficiency during the first 5cycles.

was observed, however, a significant instantaneous over-potential was observed for every cell. Figure 3c shows the voltage-time response at 1 mA.cm^{-2} for the 2.4 mol.kg^{-1} electrolyte. There are two discrete over-potentials observed during the polarization: the over-potential in the initial polarization (circled) indicates the kinetic limit of the IL system, and the second one during the final polarization (arrow) indicates a dendritic lithium morphology.[15,27] It should be noted that the over-potential decreases as the polarization continues; this was previously observed by Best and Bhatt and ascribed to the increasing geometric surface area of the electrode which meant that the actual applied current density is less than the apparent applied current density.[15,27] In conclusion, we found no significant correlation between salt concentration and lithium symmetric cell cycling performance.

Lithium Transference numbers.— The transference number is the fraction of current transported by Li^+ in an electrolyte and, possibly, the most important quantity for lithium batteries.[35–37] It is desirable for electrolytes to have a transference number of unity.[1] The traditional method to determine a transference number is the Hittorf method[38] and in this method, constant current is applied, and the changes in voltage with time are used to compare the effective charge carried to the applied charge. However, this method cannot be directly applied to an electrolyte which consists of several ionic species, or where there is growing passivation film on the electrode which affects potential. Initially, when a symmetrical cell is polarized, all positive ions (Li^+, C_3mpyr^+ in this experiment) migrate toward the negatively polarized electrode, while negative ions migrate toward the positively polarized electrode. However, after a certain time a steady state is reached and a charge concentration gradient is established, where only Li^+ moves toward the opposite electrode. By measuring the initial and steady state currents, the portion of the charge carried by Li^+ can be obtained. Considering the solution concentration gradient and the increasing passivation layer, Bruce, Evans and Vincent demonstrated that an ion transference number in a symmetric cell can be calculated as;[30,38]

$$t_{Li}^{+} = \frac{I_S(\Delta V - I_0 R_0)}{I_0(\Delta V - I_S R_S)} \quad [1]$$

where, ΔV is the potential applied across the cell, $t_{Li}{}^+$ is the lithium transference number, I_0 and I_S are the initial and steady state currents during the polarization, and R_0 and R_S are the initial and steady state resistances of the passivation layers. The authors applied this equation to polymer electrolyte systems, but subsequent researchers have shown that the equation can be adapted to ionic liquid electrolytes, where stable passivation layers form.[39–41] This equation may be used by applying a constant voltage, and measuring the initial and steady state currents, along with the resistance of the passivation film before and after the polarization. Due to the stability of the IL electrolyte toward the Li metal electrode, we show that the impedance change

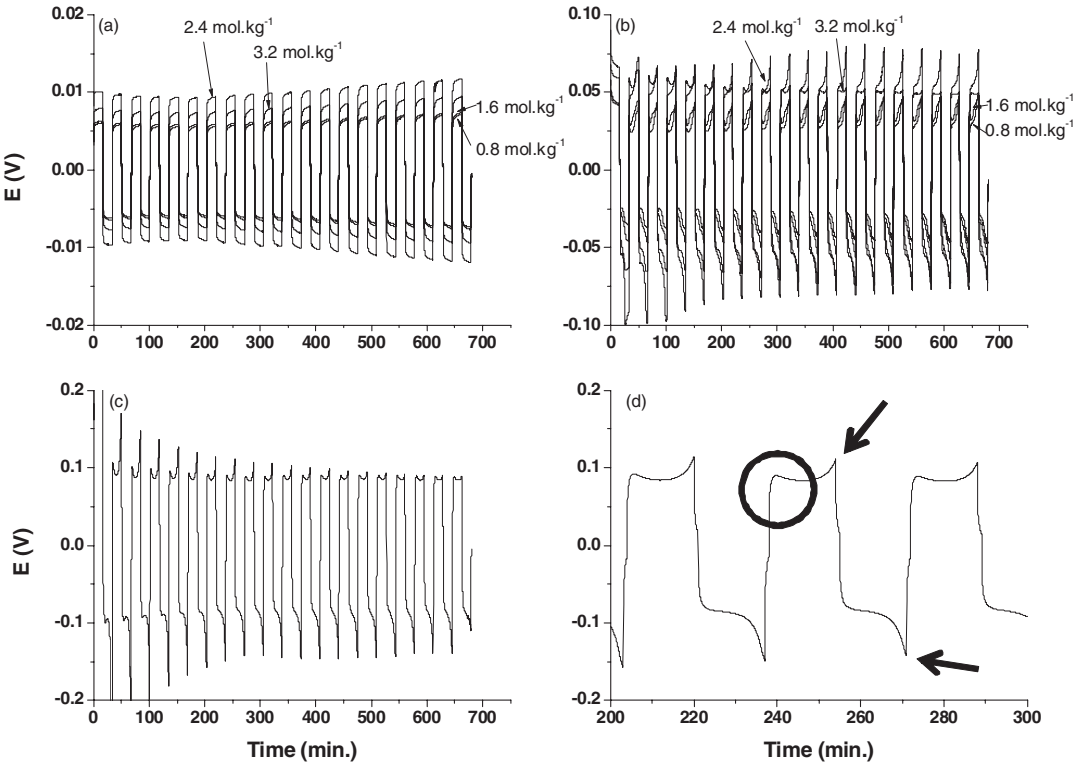

Figure 3. Voltage-time profiles for Li symmetric cells: a) 0.01 mA.cm^{-2} for 4 different electrolyte concentrations, b) 0.1 mA.cm^{-2} for 4 different electrolyte concentrations, c) 1.0 mA.cm^{-2} for 2.4 mol.kg^{-1} electrolyte, d) magnification of c).

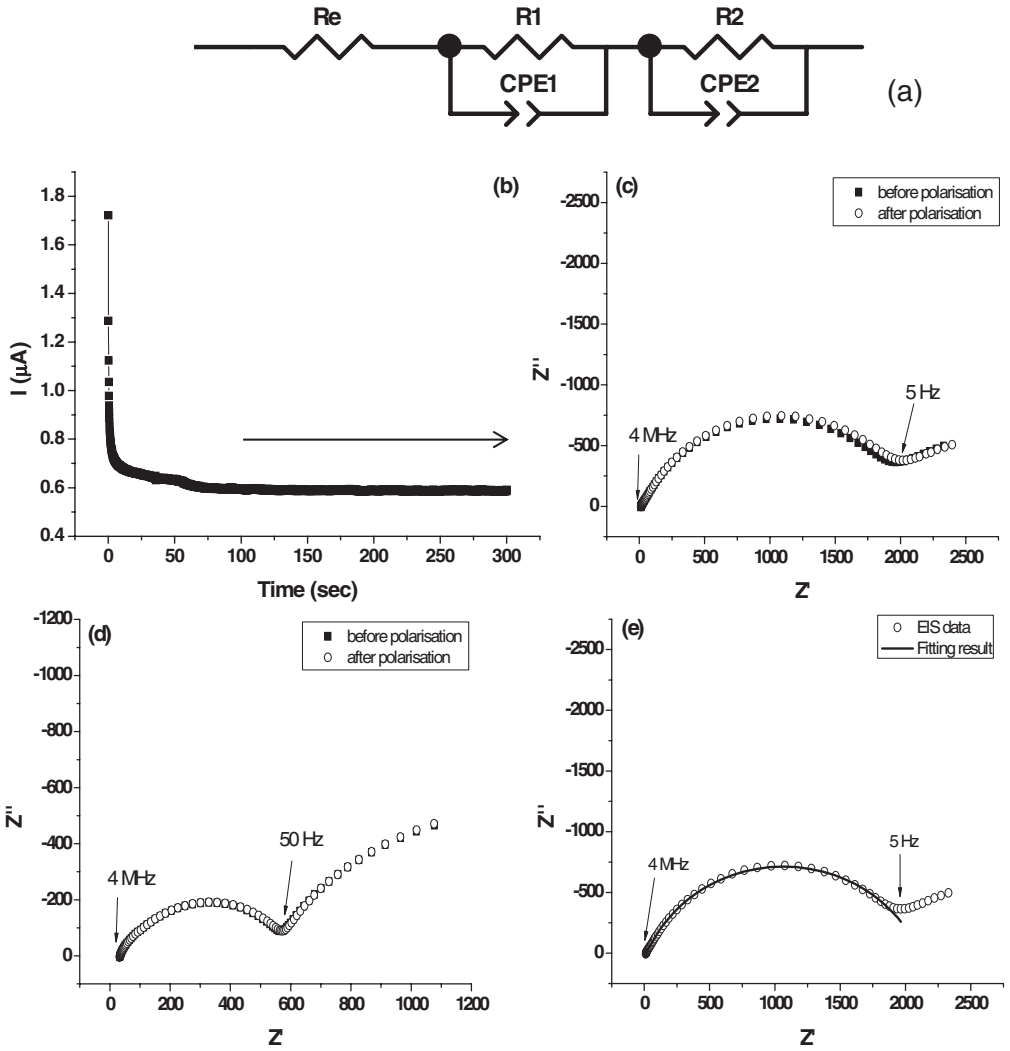

Figure 4. Polarization and EIS of Li symmetric cells. (a) Equivalent circuit used to determine electrode resistances (b) a cell reaching a steady state current. (c) EIS of 0.8 mol.kg^{-1} LiFSI in C_3mpyrFSI (d) EIS of 3.2 mol.kg^{-1} LiFSI in C_3mpyrFSI. (e) EIS of the cell used in figure (b), taken before the cell was polarized; fit to equivalent circuit in (a) also shown.

of the bulk electrolyte before and after the polarization is negligible, which allows us to use this simplified approach with confidence.

To determine the resistances of passivation layers before and after polarization, an equivalent circuit proposed by Zugmann et al. was used (as shown in Figure 4a).[37]

Figure 4b is an example of the polarization of a symmetrical cell containing 0.8 mol.kg^{-1} LiFSI in C_3mpyr FSI for 300 seconds. In contrast with previous studies on PEO or plastic crystal electrolytes, which required several hours to reach steady state current, the cells reached steady state current within several minutes. In some cells, particularly those with lower Li salt concentration (0.8 mol.kg^{-1}), an increase in current was observed after the cell had been at steady state for some time (Figure 4d). This phenomenon was not observed in the cells with the highest lithium concentrations (3.2 mol.kg^{-1}). This may be due to the presence of an unexpected side reaction on the lithium surface when the concentration of Li^+ is not sufficient. To determine I_0 and I_S, any cells which showed increasing current after steady state, did not reach steady state or showed short circuit behavior were eliminated, and the remaining cells were used to calculate the average values for each electrolyte concentration. Figure 4c is an example EIS of a Li symmetric cell containing 0.8 mol.kg^{-1} Li salt in the IL electrolyte, while 4e shows the EIS of a cell containing 3.2 mol.kg^{-1} Li salt. With increasing concentration, R_e increases from 7–8 Ω in 0.8 mol.kg^{-1} to 28–32 Ω in 3.2 mol.kg^{-1}, while the $R_1 + R_2$ value decreases from approximately 2,000 Ω in 0.8 mol.kg^{-1} to 600 Ω in 3.2 mol.kg^{-1}. This implies that the passivation layer formed on the lithium electrodes depends strongly on the concentration of Li^+, and that an increase in Li^+ concentration reduces the surface impedance. The cells were polarized at 1.0 mV for 2 hours 3 times. It should also be noted that the EIS did not change significantly after these polarizations.

The calculated transference numbers for different salt concentrations are shown in Figure 5 (with error bars) and are collated in Table II, along with conductivities, viscosities, and densities at 25°C. The density and viscosity increase, and the ionic conductivity decreases, with increasing salt concentration. The transference numbers vary from 0.1 to 0.2 as the LiFSI concentration changes. There is a general trend that increasing the salt concentration increases the

Table II. Transference numbers of each concentrated Li^+ electrolyte at 25°C.

Salt concentration	δ (g.cm^{-3})	ν (cP)	σ (mS.cm^{-1})	Ave $t_{Li}{}^+$
0.8 mol.kg^{-1}	1.413	49.4	3.40	0.113
1.6 mol.kg^{-1}	1.454	85.7	2.02	0.140
2.4 mol.kg^{-1}	1.495	136	1.23	0.185
3.2 mol.kg^{-1}	1.536	253	0.821	0.183

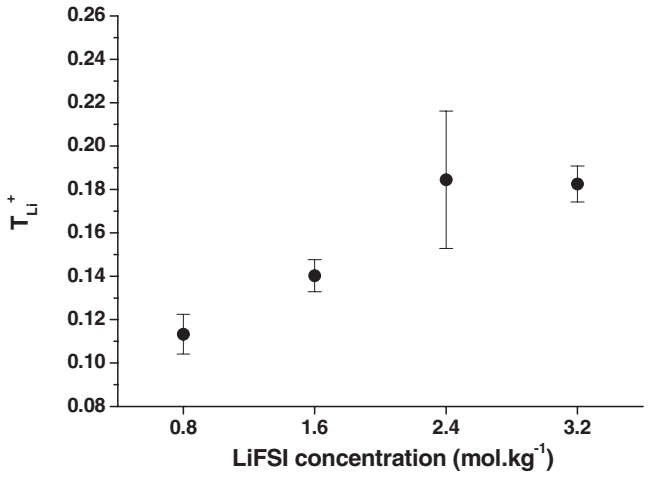

Figure 5. Li^+ transference number for different LiFSI concentrations in C_3mpyr FSI, showing average values and standard deviations.

transference number, although it is not clear if there is an optimum point between 2.4 mol.kg^{-1} and 3.2 mol.kg^{-1}. This result corresponds with that previously reported by Ferrari et al. in their *N*-methoxyethyl-*N*-methylpyrrolidinium TFSI and LiTFSI systems.[42] However, they did not explain why this result was obtained. Our measured transference numbers are similar to the 0.13 value determined by Seki et al. for 0.32 mol.kg^{-1} LiTFSI in different ILs,[41] but are much lower than the 0.6 value reported by Han et al. for a LiFSI-ammoniumFSI equimolar system[43] or the 0.4 value reported by Fernicola et al. for a TFSI-based system.[40] It should be noted that most electrolyte research has been conducted in the 0.5 mol.kg^{-1} to 1.0 mol.kg^{-1} range of added Li salts, but in some cases the optimum concentration may be much higher, as we have demonstrated here for the FSI-based electrolyte.

Li | $LiCoO_2$ cells.— First, the $LiCoO_2$ electrode pasted onto Al foil was characterized in combination with a commercial standard battery electrolyte. Cells were cycled from 2.75 V to 4.2 V at various rates between 0.1 C and 5.0 C followed by several additional cycles at 0.1 C. The initial 0.1 C charge capacity was 137 mAh.g^{-1} and discharge capacity was 131 mAh.g^{-1}, equating to 96% initial efficiency in Figure 6a, which is slightly lower than the known practical

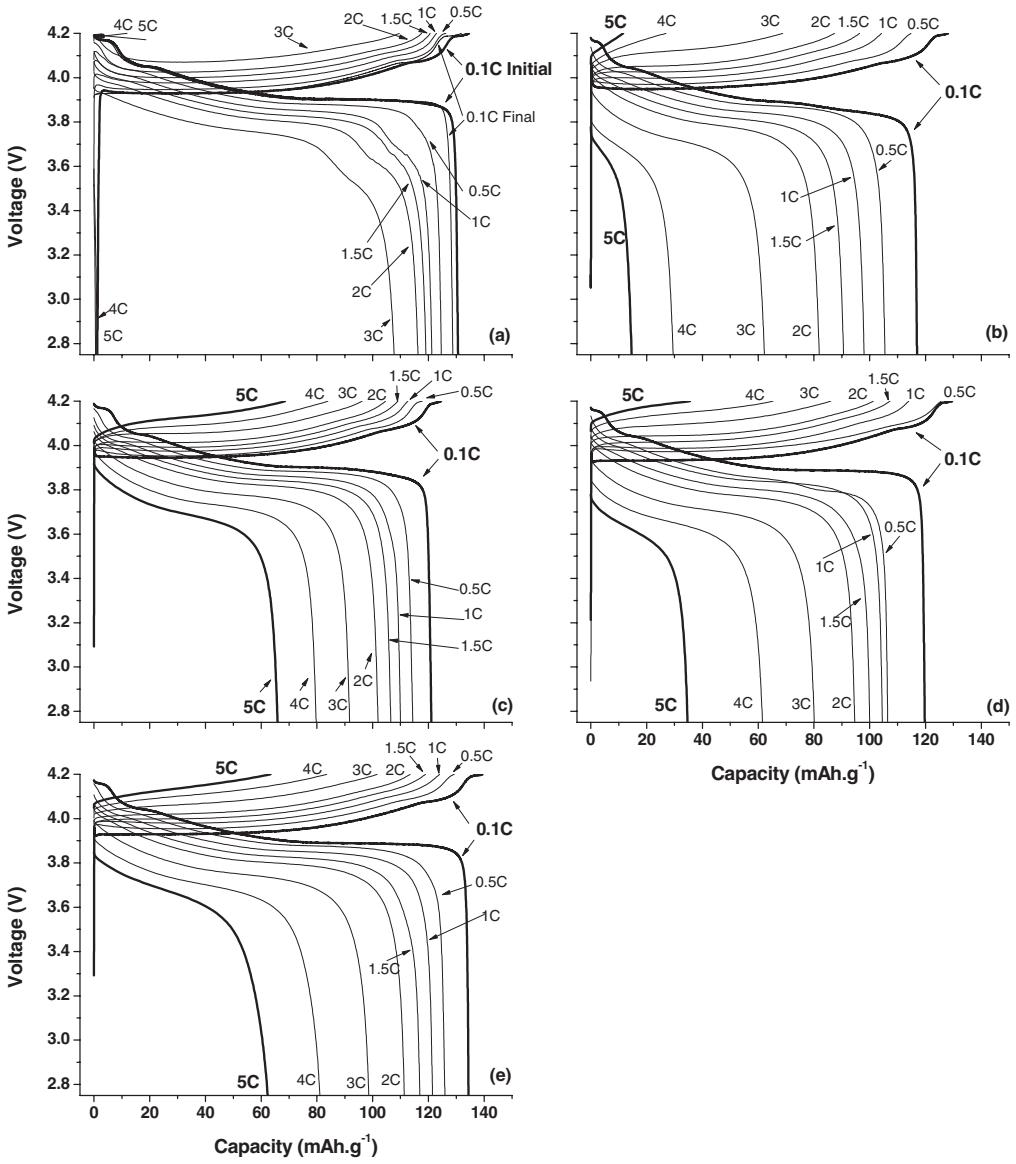

Figure 6. Charging and discharging rate capability results for Li | $LiCoO_2$ cells with Solupor 7P separator. The conditions were 0.1C, 0.2C, 0.5C, 1.0C, 1.5C, 2.0C, 3.0C, 4.0C and 5.0C rates consequently from 2.75 V to 4.2 V at room temperature. (a) 1M $LiPF_6$ in EC:DMC (50: 50 vol.%) for comparison, (b) 0.8 mol.kg^{-1}, (c) 1.6 mol.kg^{-1}, (d) 2.4 mol.kg^{-1}, (e) 3.2 mol.kg^{-1} LiFSI in C_3mpyr FSI.

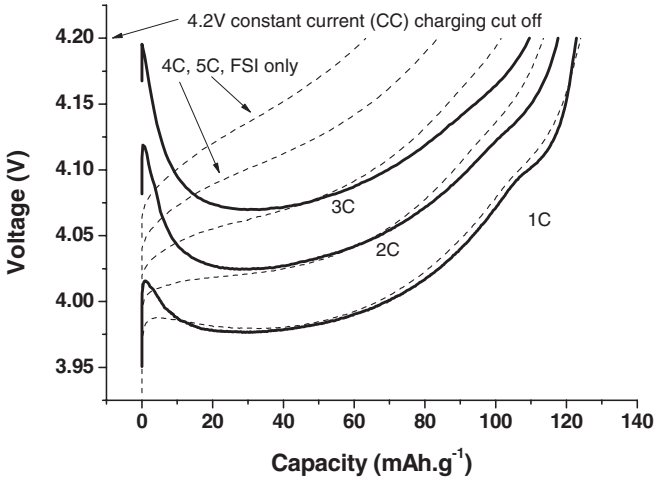

Figure 7. 1 C to 5 C Charging profiles magnified from Figure 8: Solid bold line : Organic liquid electrolyte (1M $LiPF_6$, EC:DMC = 50:50 vol.%, from Figure 8a), Dash line : 3.2 mol.kg^{-1} LiFSI in C_3mpyrFSI from Figure 8e.

capacity of $LiCoO_2$.[1,44] When the charge/discharge rate was over 1 C, a small distortion in the profile was observed in all cells, which became more noticeable at the higher rates. Of the six replicate cells tested, only one cell allowed charging up to the 3 C rate (the remaining five couldn't be charged at this rate). No cells using this standard liquid electrolyte could be charged above 4 C. These cells recovered their initial capacity when a 0.1 C rate was applied. We confirmed that the standard liquid electrolyte can be a limiting factor for high rate charge and discharge, although the actual limiting rate will vary with different electrode formulations, separators and cell configurations. Thus, in these experiments, the 3 C charging rate was the limit for the organic liquid electrolyte used, 1M $LiPF_6$ in EC:DMC (50:50 vol.%).

Figure 6b to 6e presents the results of coin cells containing C_3mpyrFSI electrolyte with different lithium salt concentrations, from 0.8 to 3.2 mol.kg^{-1}. The initial 0.1 C capacity with 0.8 mol.kg^{-1} lithium salt was 118 mAh.g^{-1}, which is lower than the standard battery electrolyte reference (Figure 6b); this can be ascribed to the higher viscosity and lower conductivity of this ionic liquid electrolyte.[20] When the salt concentration is increased to 1.6 mol.kg^{-1} (Figure 6c), surprisingly, the capacity increased to 132 mAh.g^{-1} even though the viscosity is higher and the conductivity is lower than the 0.8 mol.kg^{-1} solution. This result is in agreement with the increased current observed in the CV data previously presented in Figure 1. A decrease in capacity to 120 mAh.g^{-1} at 2.4 mol.kg^{-1} and further increase to 135 mAh.g^{-1} at 3.2 mol.kg^{-1} (Figure 6d and 6e) were also seen.

The 2 C rate capacity in the 0.8 mol.kg^{-1} electrolyte was also inferior to that of the organic liquid reference. However, the performance improved when the lithium salt concentration was increased to 1.6 mol.kg^{-1} or higher. The capacity reached the same charge and discharge capacity within a tolerance range at 3 C. A significant difference was observed at the higher charge/discharge rates of 4 C and 5 C. Whilst no cell successfully charged at 4 C with the standard electrolyte, all cells with FSI were successfully cycled at 4 C and 5 C charge/discharge rates. When the salt concentration is 3.2 mol.kg^{-1}, 50–60 mAh.g^{-1} (or approximately 40% of the initial 0.1 C discharge capacity) was observed, as shown in Figure 6e. To put these results in perspective, Matsumoto et al. conducted similar experiments using a C_3mpyr FSI ionic liquid with 0.3 mol.kg^{-1} LiTFSI,[9] however, their results showed approximately 35 mAh.g^{-1} discharge capacity at the 3 C rate with a 1.0–1.5 mg.cm^{-2} $LiCoO_2$ loading (i.e., 3 C current density is 0.42 mA.cm^{-2} to 0.81 mA.cm^{-2})[9,45] compared to the approximately 4.5 mg.cm^{-2} loading used in this work (i.e., 3 C current density is 2.43 mA.cm^{-2}). This clearly demonstrates the superior results of this work with significantly higher active material loading and salt concentrations.

The 1 C to 5 C charging profiles from Figure 6a and 6e are presented in Figure 7 for comparative purposes. The cell with the standard organic electrolyte showed significantly higher over-voltage at the high charging rates at the initial stage; this over-voltage caused by the coin cell impedance, caused the cell voltage to reach 4.2 V instantaneously, resulting in a premature end of the charging step. Additional cells were prepared and cycled with different charging method to verify the low rate capability of organic electrolyte at high current rate is only of the observed over-voltage. The discharging rate capability of the cells with a fixed low current (0.1C) charging rate is presented in Figure 8. Figure 8a is the discharging profiles with the standard organic electrolyte. It was shown that the charging profiles vary with cycles and the efficiency (discharging capacity / charging capacity) at the 5C rate charging and discharging is much greater than 100%, which was due to the remaining capacity of the previous cycle (4C) discharge. It is interesting that the cell with the standard organic electrolyte shows relatively low discharge rate capability at high C rate over 4C than the cell having FSI IL based electrolyte (Figure 8b). This implies that the relatively low discharge capability of the cell with standard organic electrolyte is not only the problem of over-voltage during high rate charging, but also of its intrinsic characteristics. Considering charging rate limit caused by over-voltage problem, since the cell impedance is high for the coin cells in this study, the charging rate limit in this study may be relatively low when compared to commercial lithium ion batteries. However, the cells using the FSI based electrolyte, which have the same configuration as the cell with standard electrolyte, do not show this over-voltage behavior at the start of charging in spite of its higher viscosity. This indicates that the Li^+ transport mechanism may be different in the ionic liquid electrolyte compared to the

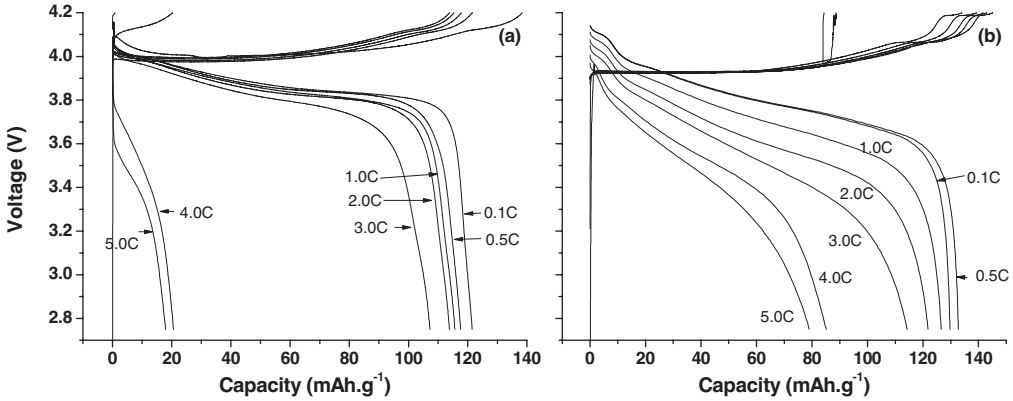

Figure 8. 0.1 C to 5 C discharging rate capability results with fixed 0.1C rate charging for Li | $LiCoO_2$ cells with Solupor 7P separator; (a) 1M $LiPF_6$ in EC:DMC (50: 50 vol.%) for comparison, (b) 3.2 mol.kg^{-1} LiFSI in C_3mpyr FSI.

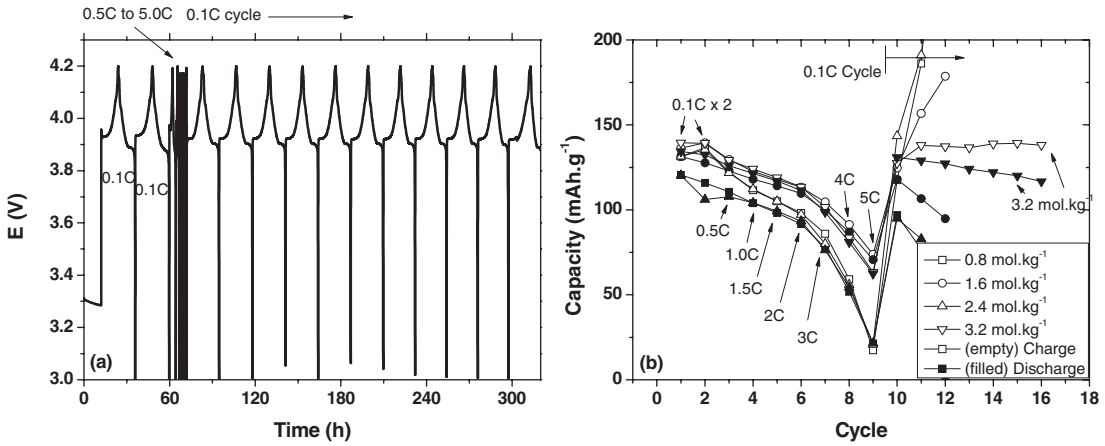

Figure 9. (a) A cycle profile of a Li | $LiCoO_2$ coin cell with 3.2 mol.kg^{-1} LiFSI in C_3mpyr FSI electrolyte, (b) Charge/discharge capacity of cells during cycling.

standard organic electrolyte. We will elaborate on this further in our forthcoming paper.

After the rate capacity measurement, the cell with 3.2 mol.kg^{-1} Li salt FSI electrolyte was cycled successfully, as shown in Figure 9a. However, the cells with lower lithium concentrations show significant capacity fade during cycling. Most of the cells containing 0.8 mol.kg^{-1} to 2.4 mol.kg^{-1} Li salt did not survive beyond 5 cycles at 0.1 C after the tests at 5 C, but the 3.2 mol.kg^{-1} cycled more reliably as shown in Figure 9b. The cells with lower lithium concentration electrolytes failed after cycling and could not be charged up to 4.2 V. The cells with 3.2 mol.kg^{-1} Li salt also showed a continuous decrease in discharge capacity after 5 C cycling. This phenomenon may be due to consumption of lithium ions during the high rate charge and discharge, or may due to degradation of the prepared $LiCoO_2$ electrode in the presence of the IL.[46] Further investigations will be performed to understand this phenomenon. The important point here is that the barrier to high rate charging and discharging because of transport limitations in the cell, as was observed when using a conventional organic liquid electrolyte system, is overcome in the FSI system. We expect this FSI system to show even better rate performance when combined with high rate cathode and anode materials.

Conclusions

We describe ionic liquid electrolytes, based on the bis(fluorosulfonyl)imide (FSI) anion with LiFSI salts, that show high rate charge and discharge characteristics. The C_3mpyrFSI ionic liquid can dissolve lithium salt up to a 1:1 IL:Li salt concentration ratio; this concentrated electrolyte then allows the Li metal electrode to be cycled at high current density. Transference numbers have also been measured in these cells to determine the lithium salt concentration effect on lithium cell performance. There is a concomitant increase in transference number from 0.1 to 0.2 with increasing salt concentration.

Li | $LiCoO_2$ batteries, prepared using this FSI electrolyte, show better rate capability than those made with 1M $LiPF_6$ in EC:DMC organic liquid electrolyte at higher than 3C charge and discharge rates, in spite of the significantly higher viscosity and lower conductivity of the IL. Importantly, the electrolyte containing 3.2 mol.kg^{-1} Li salt (i.e., a 1:1 molar ratio of salt and IL) showed the best high-rate cycling performance. This implies that the lithium transport mechanism in these high lithium concentration IL electrolytes may be different, to allow high rate charge and discharge. Finally, we expect this FSI system to show better charge and discharge capability when combined with a fast-charging electrode material.

Acknowledgments

We thank the ARC (Australian Research Council) for funding this research as part of Discovery Project DP0986205 and for Fellowship funding for DRM (Federation Fellowship) and MF (Laureate Fellowship). We also acknowledge CSIRO's National Research Flagship Energy Transformed for supporting this work. The authors also thank Dr. Tony Hollenkamp and Dr. Anand Bhatt (CSIRO) for fruitful discussions on this manuscript.

References

1. J. B. Goodenough and Y. Kim, *Chemistry of Materials*, **22**, 587 (2010).
2. H. Ohno, in *Electrochemical Aspects of Ionic Liquids*, O. Hiroyuki Editor, p. 1 (2005).
3. A. I. Bhatt, G. A. Snook, G. H. Lane, R. J. Rees, and A. S. Best, *Application of Room Temperature Ionic Liquids in Lithium Battery Technology*, Nova Science Publishers, inc (2011).
4. G. B. Appetecchi, G. T. Kim, M. Montanina, M. Carewska, R. Marcilla, D. Mecerreyes, and I. De Meatza, *J. Power Sources*, **195**, 3668 (2010).
5. S. F. Lux, M. Schmuck, S. Jeong, S. Passerini, M. Winter, and A. Balducci, *Int. J. Energy Res.*, **34**, 97 (2010).
6. G. T. Kim, S. S. Jeong, M. Z. Xue, A. Balducci, M. Winter, S. Passerini, F. Alessandrini, and G. B. Appetecchi, *J. Power Sources*, **199**, 239 (2012).
7. K. Zaghib, P. Charest, A. Guerfi, J. Shim, M. Perrier, and K. Striebel, *J. Power Sources*, **134**, 124 (2004).
8. M. Ishikawa, T. Sugimoto, M. Kikuta, E. Ishiko, and M. Kono, *J. Power Sources*, **162**, 658 (2006).
9. H. Matsumoto, H. Sakaebe, K. Tatsumi, M. Kikuta, E. Ishiko, and M. Kono, *J. Power Sources*, **160**, 1308 (2006).
10. A. Guerfi, S. Duchesne, Y. Kobayashi, A. Vijh, and K. Zaghib, *J. Power Sources*, **175**, 866 (2008).
11. J. Saint, A. S. Best, A. F. Hollenkamp, J. Kerr, J. H. Shin, and M. M. Doeff, *J. Electrochem. Soc.*, **155**, A172 (2008).
12. S. Seki, Y. Kobayashi, H. Miyashiro, Y. Ohno, Y. Mita, N. Terada, P. Charest, A. Guerfi, and K. Zaghib, *J. Phys. Chem. C*, **112**, 16708 (2008).
13. Q. Zhou, W. A. Henderson, G. B. Appetecchi, M. Montanino, and S. Passerini, *J. Phys. Chem. B*, **112**, 13577 (2008).
14. E. Paillard, Q. Zhou, W. A. Henderson, G. B. Appetecchi, M. Montanino, and S. Passerini, *Journal of the Electrochemical Society*, **156**, A891 (2009).
15. A. S. Best, A. I. Bhatt, and A. F. Hollenkamp, *J. Electrochem. Soc.*, **157**, A903 (2010).
16. A. Lewandowski and I. Acznik, *Electrochimica Acta*, **56**, 211 (2010).
17. Y. D. Wang, K. Zaghib, A. Guerfi, F. F. C. Bazito, R. M. Torresi, and J. R. Dahn, *Electrochim. Acta*, **52**, 6346 (2007).
18. A. Abouimrane, J. Ding, and I. J. Davidson, *J. Power Sources*, **189**, 693 (2009).
19. R. Vijayaraghavan, M. Surianarayanan, V. Armel, D. R. MacFarlane, and V. P. Sridhar, *Chem. Commun.*, 6297 (2009).
20. S. Seki, Y. Ohno, Y. Kobayashi, H. Miyashiro, A. Usami, Y. Mita, H. Tokuda, M. Watanabe, K. Hayamizu, S. Tsuzuki, M. Hattori, and N. Terada, *J. Electrochem. Soc.*, **154**, A173 (2007).
21. A. Nyman, M. Behm, and G. Lindbergh, *Electrochim. Acta*, **53**, 6356 (2008).
22. J. H. Shin, W. A. Henderson, G. B. Appetecchi, F. Alessandrini, and S. Passerini, *Electrochim. Acta*, **50**, 3859 (2005).
23. S. Randstroem, G. B. Appetecchi, C. Lagergren, A. Moreno, and S. Passerini, *Electrochim. Acta*, **53**, 1837 (2007).

24. M. Aklalouch, J. Manuel Amarilla, R. M. Rojas, I. Saadoune, and J. Maria Rojo, *J. Power Sources*, **185**, 501 (2008).
25. A. Abouimrane, I. Belharouak, and K. Amine, *Electrochemistry Communications*, **11**, 1073 (2009).
26. R. Marom, S. F. Amalraj, N. Leifer, D. Jacob, and D. Aurbach, *J. Mater. Chem.*, **21**, 9938 (2011).
27. A. I. Bhatt, A. S. Best, J. Huang, and A. F. Hollenkamp, *J. Electrochem. Soc.*, **157**, A66 (2010).
28. H. H. Girault, *Analytical and physical electrochemistry*, p. xiii + 431 pp. (2004).
29. G. A. Snook, A. S. Best, A. G. Pandolfo, and A. F. Hollenkamp, *Electrochem. Commun.*, **8**, 1405 (2006).
30. J. Evans, C. A. Vincent, and P. G. Bruce, *Polymer*, **28**, 2324 (1987).
31. P. G. Bruce and C. A. Vincent, *Journal of the Chemical Society-Faraday Transactions*, **89**, 3187 (1993).
32. R. Wibowo, S. E. W. Jones, and R. G. Compton, *J. Phys. Chem. B*, **113**, 12293 (2009).
33. P. C. Howlett, E. I. Izgorodina, M. Forsyth, and D. R. MacFarlane, *Z. Phys. Chemie-Int. J. Res. Phys. Chem. Chem. Phys.*, **220**, 1483 (2006).
34. G. Nagasubramanian, *Int. J. Electrochem. Sci.*, **2**, 913 (2007).
35. P. W. Atkins, *Physical chemistry*, Oxford University Press, Oxford (1998).
36. H. Hafezi and J. Newman, *J. Electrochem. Soc.*, **147**, 3036 (2000).
37. S. Zugmann, M. Fleischmann, M. Amereller, R. M. Gschwind, H. D. Wiemhoefer, and H. J. Gores, *Electrochimica Acta*, **56**, 3926 (2011).
38. P. G. Bruce, M. T. Hardgrave, and C. A. Vincent, *Solid State Ion.*, **53**, 1087 (1992).
39. K. M. Abraham, Z. Jiang, and B. Carroll, *Chem. Mat.*, **9**, 1978 (1997).
40. A. Fernicola, F. Croce, B. Scrosati, T. Watanabe, and H. Ohno, *J. Power Sources*, **174**, 342 (2007).
41. S. Seki, Y. Ohno, H. Miyashiro, Y. Kobayashi, A. Usami, Y. Mita, N. Terada, K. Hayamizu, S. Tsuzuki, and M. Watanabe, *J. Electrochem. Soc.*, **155**, A421 (2008).
42. S. Ferrari, E. Quartarone, P. Mustarelli, A. Magistris, S. Protti, S. Lazzaroni, M. Fagnoni, and A. Albini, *J. Power Sources*, **194**, 45 (2009).
43. H.-B. Han, K. Liu, S.-W. Feng, S.-S. Zhou, W.-F. Feng, J. Nie, H. Li, X.-J. Huang, H. Matsumoto, M. Armand, and Z.-B. Zhou, *Electrochimica Acta*, **55**, 7134 (2010).
44. K. Mizushima, P. C. Jones, P. J. Wiseman, and J. B. Goodenough, *Mater. Res. Bull.*, **15**, 783 (1980).
45. H. Sakaebe and H. Matsumoto, *Electrochem. Commun.*, **5**, 594 (2003).
46. G. A. Snook, T. D. Huynh, A. F. Hollenkamp, and A. S. Best, *J. Electroanal. Chem.*, **687**, 30 (2012).